

Significant Results:

RF superconductivity: Research supported by this project led to the following significant results:

- We have found strong evidence that the electron mean free path plays an important role in the surface resistance of SRF materials. Beyond the well-known minimization of the low-field BCS resistance for mean free path values near half the clean coherence length, this role is twofold: decreasing the mean free path into the dirty limit causes an increasingly strong anti-Q-slope, resulting in very low BCS resistances at technologically interesting accelerating gradients (see Fig. SRF1), but it also increases susceptibility to increases in the effective residual resistance due to trapped magnetic flux (see Fig. SRF2). We have drawn a theoretical connection between the observed dependence on mean free path of the field-dependent BCS resistance and the overheating of quasiparticles, which increases linearly with mean free path in the dirty limit. This is linked either to a decreasing energy transfer rate from quasiparticles to phonons or to an additional energy loss channel from quasiparticles due to elastic scattering on impurities which decreases as the mean free path increases. We have used this model to calculate the BCS resistance for short-mean-free-path cavities at operating accelerator gradients, and combined this with theoretical results for the flux-trapping sensitivity to find an optimal mean free path for a given technologically achievable trapped flux. This work allows for determining optimal SRF cavity treatment protocols for very high efficient (high Q0) SRF cavities for future accelerators, and had strongly impacted the LCLS-II SRF linac design.
- We have used nitrogen doping of niobium cavities to systematically adjust the mean free path (i.e. κ) of the RF penetration layer and have measured the impact on maximum surface fields (quench fields); see Fig. SRF3. We found that reliable high κ SRF cavity operation at metastable fields above the lower critical magnetic field can be achieved if large surface defects are avoided. We also demonstrated that operating fields well above the lower critical fields can reliably be achieved in high κ ($\kappa > 40$) Nb₃Sn cavities; see Fig. SRF4. An EDX map of a sample cut-out taken from a Nb₃Sn cavity from a region that showed substantial heating during RF testing showed

coatings of insufficient thickness (~200 nm instead of the nominal 3000 nm); see Fig. SRF4. Together with the tin-depleted regions found previously, these thin coating regions are likely sources increasing low temperature surface resistance and possibly causing quench above the lower critical field, but well below the ultimate field limit set by the superheating field.

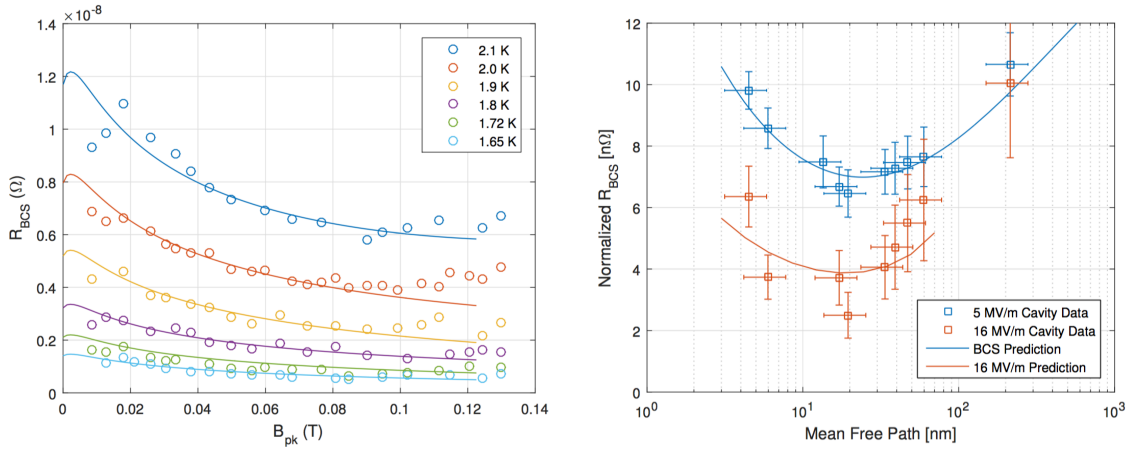


Figure SRF1: Left: Measured BCS surface resistance of a nitrogen doped 1.3GHz SRF cavity (mean free path = 34 nm) vs peak surface magnetic field. Lines show fitted theoretical predictions based on theoretical work by A. Gurevich [Phys. Rev. Lett., 113:087001, Aug 2014] with given overheating parameter. Right: BCS resistance at 2 K and 1.3 GHz as a function of mean free path. Blue points and curves are low field data, taken at 5 MV/m (21 mT). Red points are the experimental data at 16 MV/m (68 mT), and the lower red curve is the theoretical BCS resistance extrapolated to 16 MV/m by the modified mean-free-path-dependent theory.

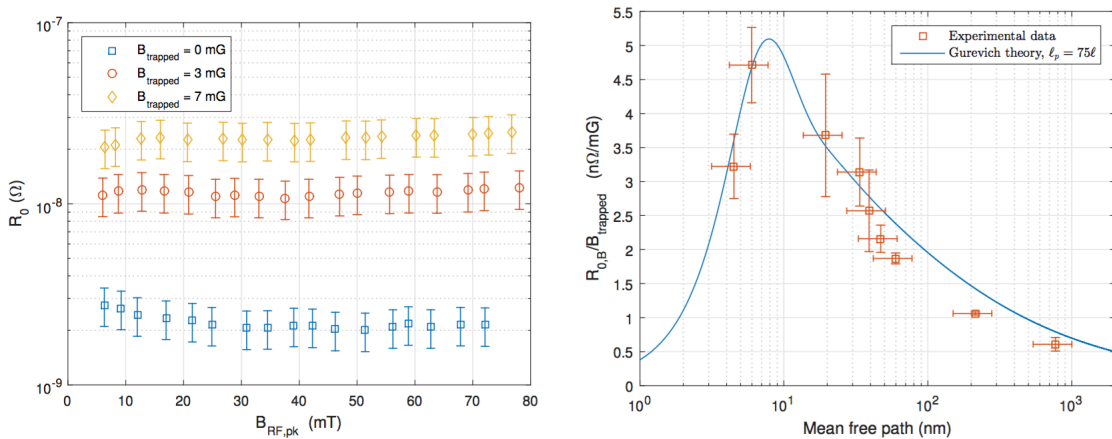


Figure SRF2: Left: Representative residual surface resistance vs. peak magnetic

surface field for a 1.3 GHz TESLA cavity, at varying levels of trapped magnetic flux. Right: Experimental data and theoretical prediction for sensitivity of residual resistance to trapped magnetic flux as a function of mean free path.

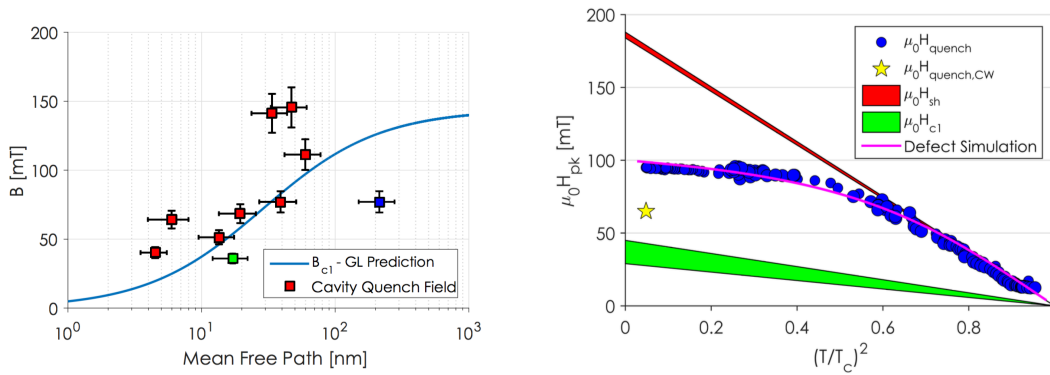


Figure SRF3: Left: Predicted lower critical field B_{c1} from GL theory versus mean free path and the nitrogen-doped niobium cavity quench fields (converted to the peak magnetic field on the cavity surface), from CW testing. The point in blue is most likely limited by multipacting and the point in green by normal conducting NbN on the surface due to only a small amount of final etch after nitrogen-doping. Right: Peak surface magnetic field vs $(T/T_c)^2$ for a small κ , nitrogen doped SRF cavity. Near T_c , quench field follows the superheating field B_{sh} . However, at lower temperatures, quench field is significantly lower than B_{sh} but still well above B_{c1} , consistent with a quench at a defect. CW quench field is also shown and can be seen to be significantly higher than B_{c1} . B_{c1} and B_{sh} were calculated from extracted mean free path values obtained from CW RF measurements.

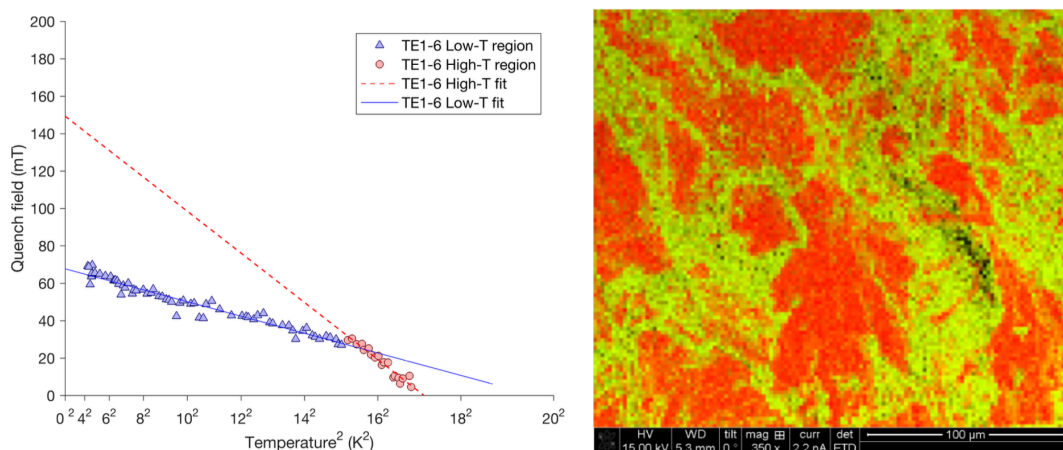


Figure SRF4: Left: Peak surface magnetic field (quench field) as a function of temperature for a Nb3Sn cavity vs temperature in high-pulsed-power operation.

All quenches happened above H_{c1} , the lower critical field. Right: An EDX map taken at 25 kV on the FEI Strata 400 SEM from a sample cut-out taken from Nb₃Sn cavity ERL1-5. This cut-out was taken from a region that showed substantial heating during RF testing, as seen from temperature mapping. Areas show in red have Nb₃Sn coatings of insufficient thickness.